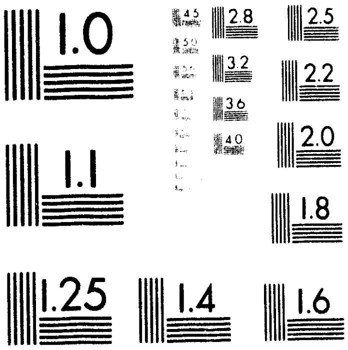
1.0
4.5
5.0
2.8
2.5
3.2
2.2
3.6
4.0
2.0
1.1
1.8
1.25
1.4
1.6

1 of 1

ANL/ET/CP--78725
Conf-931142--4

GRAIN BOUNDARY DEGRADATION OF YBCO SUPERCONDUCTORS SINTERED IN CO_2–CONTAINING ATMOSPHERES*

U. Balachandran, K. L. Merkle,[+] and J. N. Mundy[+]
Energy Technology Division
[+]Materials Science Division
Argonne National Laboratory
Argonne, IL 60439

Y. Gao
Department of Materials and Metallurgical Engineering
New Mexico Institute of Mining and Metallurgy
Socorro, NM 87801

C. Zhang, D. Xu, and G. Selvaduray
Department of Materials Engineering
San Jose State University
San Jose, CA 95192

November 1993

Paper submitted for publication in the Proc. of the International Symposium on Grain Boundaries and Interfacial Phenomena in Electronic Ceramics, The 1993 PAC RIM Meeting, November 7-10, 1993, Honolulu, HI.

*Work supported by the U.S. Department of Energy, Energy Efficiency and Renewable Energy, as part of a program to develop electric power technology, Basic Energy Sciences-Materials Science, under Contract W-31-109-Eng-38; and the National Science Foundation (DMR88-09854) through the Science and Technology Center for Superconductivity.

GRAIN BOUNDARY DEGRADATION OF YBCO SUPERCONDUCTORS SINTERED IN CO_2-CONTAINING ATMOSPHERES

U. Balachandran, K. L. Merkle,+ and J. N. Mundy+
Energy Technology Division
+Materials Science Division
Argonne National Laboratory
Argonne, IL 60439

Y. Gao
Department of Materials and Metallurgical Engineering
New Mexico Institute of Mining and Metallurgy
Socorro, NM 87801

C. Zhang, D. Xu, and G. Selvaduray
Department of Materials Engineering
San Jose State University
San Jose, CA 95192

ABSTRACT

The transport critical current density (J_c) of YBCO superconductors decreased with increasing CO_2 partial pressure in the sintering atmosphere and ultimately reached zero, even though magnetization measurements showed that the bulk of the samples with zero J_c remained superconducting. The microstructure and composition of the samples was investigated by high resolution transmission electron microscopy and secondary-ion mass spectroscopy (SIMS). Microbeam SIMS indicated carbon segregation at grain boundaries (GBs). Approximately 10% of the GBs were coated with a thin layer of a second phase, deduced to be $BaCuO_2$ and $BaCu_2O_2$. Near some grain boundaries, the structure was tetragonal within several tens of nm of the boundaries. The degradation of J_c is discussed in terms of the partial pressure of CO_2 and the processing temperatures. Detailed examination of GB microstructures is given in this paper.

INTRODUCTION

A major limitation of the bulk processed $YBa_2Cu_3O_{7-x}$ (YBCO) superconductor for practical applications is the very low value of the transport critical current density (J_c). A possible cause of this problem is blockage of the superconducting currents across the grain boundaries. One type of blockage is the structural discontinuity at grain boundaries [1,2]. Another possible blockage is the presence of second phases at grain boundaries [3-5]. Nakahara et al. [6] reported the presence of a few angstrom thick second phase at grain boundaries. By using scanning Auger microscopy, Verhoeven et al. [7] concluded that the second phase is a BaCO3 and that the carbon contamination was not a product of original processing, but a consequence of the environment.

The transition temperature, J_c, and width of superconducting transition of YBCO are influenced by atmospheric contaminants such as CO_2 and H_2O [4,5,8-10]. There are two potential sources of CO_2 during YBCO are processed. One source is the CO_2 contained in the oxygen gas used during sintering and/or annealing. Another source is the CO_2 derived from the decomposition of $BaCO_3$ during calcination step. Each source affects the quality of the final product in different ways and can lead to a drop in the J_c. During calcination, the Y_2O_3, $BaCO_3$, and CuO powders react to form YBCO. When $BaCO_3$ decomposes, CO_2 is released. The localized concentration of CO_2 can quickly reach its equilibrium value, and stagnant regions of CO_2 can form, even in systems with flowing gases. This localized CO_2 pressure, depending on the temperature and other thermodynamic conditions, can cause other decomposition reactions, thereby forming undesired phases, which in turn contribute to reduce the J_c of the final product. A dynamic low-pressure vacuum calcination technique has been developed by Balachandran et al. [11,12] to remove the CO_2 effectively from the reaction chamber during calcination of precursors to form YBCO. Reaction of YBCO with CO_2 present in the sintering atmosphere has been reported by several researchers [3-5,8,13]. Gallagher et al. [8] reported that at 1000°C in a 1% CO_2/99% O_2 mixture, the YBCO phase was not decomposed, while in a 10% CO_2/90% O_2 mixture the YBCO phase was completely decomposed, forming $BaCO_3$, $Y_2Cu_2O_5$, and CuO. Fjellvag et al. [13] studied the interaction between CO_2 and YBCO in a 0.1% CO_2/99.9% O_2 mixture and reported that the reaction occurred in two steps: below 730°C the reaction products are $BaCO_3$, Y_2O_3, and CuO, while above this temperature the products are $BaCO_3$, $Y_2Cu_2O_5$, and CuO. Because of limitations of the X-ray diffraction technique, neither Gallagher et al. [8] nor Fjellvag et al. [13] were able to study the spatial origin of the reaction between YBCO and CO_2, which may be very important with regard to the low value of the J_c found in ceramic superconductors. Recently Cooper et al. [14] used in-situ electrical conductivity measurements to study the kinetics of YBCO decomposition in a flowing 5% CO_2/95% O_2 atmosphere at 815°C.

In this paper, we report on the degradation of J_c of YBCO sintered in CO_2-containing atmospheres. The grain boundary microstructures and compositions of the samples were investigated by transmission electron microscopy (TEM), analytical electron microscopy (AEM), and secondary ion mass spectroscopy (SIMS). The relationships between the properties and the partial pressure of CO_2 are discussed in terms of microstructural changes.

EXPERIMENTAL

Phase-pure orthorhombic powders of YBCO were prepared by mixing and grinding stoichiometric amounts of Y_2O_3, $BaCO_3$, and CuO and then calcining in flowing oxygen at a reduced total pressure of ≈2 mm Hg at about 850°C; this was followed by low-temperature annealing in ambient-pressure oxygen [11,12]. The reduced pressure used in this process ensured the efficient removal of the CO_2 gas generated during the formation of the YBCO phase and resulted in the production of phase-pure orthorhombic powders. These powders were pressed into small pellets and sintered for ≈5 h in flowing CO_2/O_2 gas mixture at ≈1 atm. pressure. The portion of CO_2 in the mixtures was 0-5%. Four groups of samples were sintered at temperatures of 910, 940, 970, and 1000°C, respectively. Transition temperatures were obtained by resistivity and magnetization techniques. A low-field rf SQUID magnetometer was used for the magnetization measurements. TEM specimen discs (3 mm diameter) were cut from the bulk samples and polished on 600-grid paper in methyl alcohol to a thickness of ≈120 μm. The disks were dimpled from both sides to have a thin area with a thickness ≈25 μm at the center. The final TEM specimens were obtained by argon ion-thinning using a liquid nitrogen cooled stage. TEM observations and AEM analysis were performed utilizing a Philips 420 at an operating voltage of 120 kV.

RESULTS AND DISCUSSION

The J_c (at 77 K, self-field) values decreased with decreasing sintering temperatures and increasing CO_2 content. The Jc finally becomes zero at a CO_2 partial pressure that is dependent on the sintering temperature. Resistivity measurements showed that the materials with $J_c = 0$ were semiconductive. Figure 1 summarizes these results and presents them in terms of processing conditions, namely partial pressure of CO_2 and sintering temperature, necessary for the production of superconductors. The solid line separates the stability regions of superconductors and semiconductors. Magnetization measurements for samples with $J_c = 0$ indicated that the major phase of these samples is still superconducting. The onset of superconductivity is almost the same, ≈90 K, for all samples. The presence of CO_2 is found to be detrimental, despite the fact that the major phases are still superconducting. Figure 2 shows the example of the resistivity vs temperature and magnetization vs temperature curves for the samples sintered at 940°C in pure O_2 and in a 0.5% CO_2/99.5% O_2 mixture. For the samples with $J_c = 0$, (curve 2), the magnetization drops much more rapidly through the transition than as found for the samples with high J_c. Resistivity and magnetization measurements of samples with high and zero J_c suggests a strong blockage of superconducting current at the grain boundaries in the latter samples. A possible cause of the blockage could be a thin layer of a second phase at grain boundaries, formed during sintering due to the reaction between YBCO and CO_2 in the gas atmosphere. This hypothesis was checked by TEM examination of several samples.

The compositions at and near grain boundaries in sintered samples were investigated using TEM in conjunction with energy dispersive spectroscopy (EDS). No evidence of second phases at grain boundaries was found in samples sintered in pure O_2. However, two distinct types of grain boundaries were observed in the samples that were sintered in 0.5% CO_2/99.5% O_2 mixture. Approximately 10% of the observed grain boundaries were found to be wet by a thin layer of a second phase, as shown in Figure 3. EDS spectra obtained from locations along this boundary indicated that the composition of this layer was rich in Ba and Cu, but depleted in Y, and was likey to be $BaCuO_2$. At some locations this layer was found to be extremely rich in copper, and it is likely that the composition may be due to the eutectic reaction between $BaCuO_2$ and CuO, in accordance with the phase diagram [15]. The remaining boundaries (≈90% of the boundaries) appeared quite sharp and has no obvious evidence of secondary phases.

Because of the multitude of possible percolation paths, the value of J_c would not become zero if only 10% of the grain boundaries are coated with a second phase. Therefore, a majority of the grain boundaries have to be resistive enough to block the flow of superconducting current across the boundaries. By careful study of high-resolution electron microscopy (HREM) images, we found that the structure near the sharp grain boundaries was not orthorhombic, but tetragonal, as shown in Figure 4.

The lattice fringes in the [001] direction were clearly observed, and it was found that the spacing c was 1.19 nm near the grain boundary whereas c = 1.17 nm in the region far from the grain boundary. From neutron diffraction data [16], it is known that the structure with c = 1.19 nm is tetragonal and c = 1.17 nm is orthorhombic. Another indication of the presence of the tetragonal structure is the termination of the twin structure as marked by T in Fig. 4. This can be taken as the signature of the demarcation line between the orthorhombic and tetragonal structures, since the tetragonal structure has no twins.

A possible cause of the phase transformation from the orthorhombic to the tetragonal structure is the incorporation of carbon into the lattice due to the CO_2 in the sintering atmosphere[3-5]. Carbon diffuses into the lattice, and expells the oxygen in the orthorhombic structure, thus forming a tetragonal structure. Secondary ion mass spectroscopy (SIMS) was used to detect the carbon signal. The carbon maps obtained by SIMS show no carbon signal for the sample sintered in pure O_2, but a strong carbon signal at grain boundary regions for the samples sintered in CO_2/O_2 mixtures [3]. It should be noted that Fig. 4 is a special example which has a particularly large tetragonal region. We observed, in most cases, that such tetragonal regions near grain boundaries vary from a few nanometer to several tens of nanometers. Therefore, they were very difficult to detect and are not readily identifiable in most boundaries. The width of these tetragonal regions are much larger compared to the coherence length in this material. Therefore, it is reasonable to conclude that these second phases block the passage of superconducting current.

EDS also revealed the presence of precipitates of Y_2BaCuO_5 in the samples sintered in 0.5% CO_2/99.5% O_2 mixture, as shown in Figure 5. Based on the findings here, and the fact that the samples were phase-pure before they were sintered in CO_2 containing atmosphere, it can be concluded that the YBCO decomposes in the presence of CO_2, yielding Y_2BaCuO_5, $BaCO_3$, $BaCuO_2$, and CuO. The decomposition products depend on the temperature and partial pressure of CO_2 in the sintering atmosphere.

Our previous work indicates that the reaction rate with CO_2 can differ greatly for different grain boundaries [4]. For example, in some cases, the reaction just started at some grain boundaries, as shown in Figure 6 (a), while the reaction was complete at other grain boundaries, as indicated in Figure 6(b). The reaction rate may depend on the grain boundary misorientation, or on the grain boundary type. However, it is not clear at the moment which aspects of the grain boundary geometry or composition are controlling the nucleation and growth of secondary phases. At low partial pressures of CO_2 (up to few hundred parts per million), only a fraction of the grain boundaries may be modified sufficiently by such reactions to cause interruption of the superconducting current. For the samples sintered in 5% CO_2/95% O_2, the initial YBCO phase was found to be completely decomposed and no superconducting transition was observed. Both the EDS and XRD showed that the decomposition products were $BaCO_3$, CuO, and Y_2BaCuO_5.

CONCLUSIONS

YBCO samples react strongly with CO_2 in the sintering atmosphere, leading to a decrease in J_c. The tendency of the reaction depends on the sintering temperature, partial pressure of CO_2, and the grain boundary structure. Increasing the sintering temperatures raise the equilibrium CO_2 partial pressure. Up to a certain value of the CO_2 partial pressure, the YBCO samples gradually lose their superconducting properties, although the majority phase of these samples is still superconducting. The secondary phases formed at the grain boundaries as a result of reaction of YBCO with CO_2 blocks the flow of superconducting currents. The carbon segregation near the grain boundary regions results in a phase transformation of the orthorhombic phase to the non-superconducting tetragonal phase. At CO_2 level as high as 5%, the YBCO completely decomposes to $BaCO_3$, Y_2BaCuO_5, and CuO.

ACKNOWLEDGMENTS

Work supported by the U.S. Department of Energy, Energy Efficiency and Renewable Energy, as part of a program to develop electric power technology, Basic Energy Sciences-Materials Science, under Contract W-31-109-Eng-38; and the National Science Foundation (DMR88-09854) through the Science and Technology Center for Superconductivity.

REFERENCES

1. P. Chaudhari, J. Mannhart, D. Dimos, C. C. Tsuei, J. Chi, M. M. Oprysko, and M. Scheuermann, Phys. Rev. Lett., **60**, 1653 (1988).

2. D. Dimos, P. Chaudhari, J. Mannhart, and F. K. LeGoues, Phys. Rev. Lett., **61**, 219 (1988).

3. Y. Gao. Y. Li, K. L. Merkle, J. N. Mundy, C. Zhang, U. Balachandran, and R. B. Poeppel, Mater. Lett., **9**, 347 (1990).

4. Y. Gao, K. L. Merkle, C. Zhang, U. Balachandran, and R. B. Poeppel, J. Mater. Res. **5**, 1363 (1990).

5. G. Selvaduray, C. Zhang, U. Balachandran, Y. Gao, K. L. Merkle, H. Shi, and R. B. Poeppel, J. Mater. Res., **7**, 283 (1992).

6. S. Nakahara, G. J. Fisanick, M. F. Yan, R. B. van Dover, T. Boone, and R. Moore, J. Crystal Growth, **85**, 639 (1987).

7. J. D. Verhoeven, A. J. Bevolo, R. W. McCallum, E. D. Gibson, and M. A. Noack, Appl. Phys. Letters, **52**, 745 (1988).

8. P. K. Gallagher, G. S. Grader, and H. M. O'Bryan, Mater. Res. Bull., **23**, 1491 (1988).

9. E. K. Chang, E. F. Ezell, and M. J. Kirschner, Supercond. Sci. Technol., **8**, 391 (1990).

10. T. B. Lindemer, C. R. Hubbard, and J. Brynestad, Physica C, **167**, 312 (1990).

11. U. Balachandran, R. B. Poeppel, J. E. Emerson, S. A. Johnson, M. T. Lanagan, C. A. Youngdahl, D. Shi, K. C. Goretta, and N. G. Eror, Mater. Lett., **8**, 454 (1989).

12. U. Balachandran, R. B. Poeppel, J. E. Emerson, and S. A. Johnson, U.S. Patent 5,086,034, February 4, 1992.

13. H. Fjellvag, P. Karen, A. Kjekshus, P. Kofstad, and T. Norby, Acta Chem. Scand., **A42**, 178 (1988).

14. E. A. Cooper, A. K. Gangopadhyay, T. O. Mason, and U. Balachandran, J. Mater. Res., **6**, 1393 (1991).

15. R. A. Laudise, L. F. Schneemeyer, and R. L. Barnes, J. Cryst. Growth, **85**, 569 (1987).

16. J. D. Jorgensen, M. A. Beno, D. G. Hinks, L. Solderholm, K. J. Volin, R. L. Hitterman, J. D. Grace, I. K. Schuller, C. U. Segre, K. Zhang, and M. S. Kleefisch, Phys. Rev. **B36**, 3608 (1987).

FIGURE CAPTIONS

Figure 1: Stability of YBCO superconductor as a function of partial pressure of CO_2 (P_{CO_2}) and temperature.

Figure 2: Resistivity vs temperature (a), and magnetization vs temperature (b) for two YBCO samples sintered at 940°C (Sample 1 was sintered in pure O_2; Sample 2, in 0.5% CO_2/99.5% O_2).

Figure 3: TEM micrograph of grain boundary (GB) in YBCO sample sintered at 970°C in 0.5% CO_2/99.5% O_2 atmosphere.

Figure 4: HREM image of grain boundary (GB) in YBCO sample sintered at 970°C in 0.5% CO_2/99.5% O_2 atmosphere. Termination of the twin structure is marked by T in this figure.

Figure 5: TEM micrograph of YBCO sample sintered at 970°C in 0.5% CO_2/99.5% O_2 atmosphere. The second phases, marked S, were identified to be Y_2BaCuO_5.

Figure 6: (a) Nuclei of the secondary phases at a grain boundary in YBCO sample treated in CO_2/O_2 atmosphere for 0.5 h; (b) Some grain boundaries are completely coated with secondary phases in the same sample as in (a).

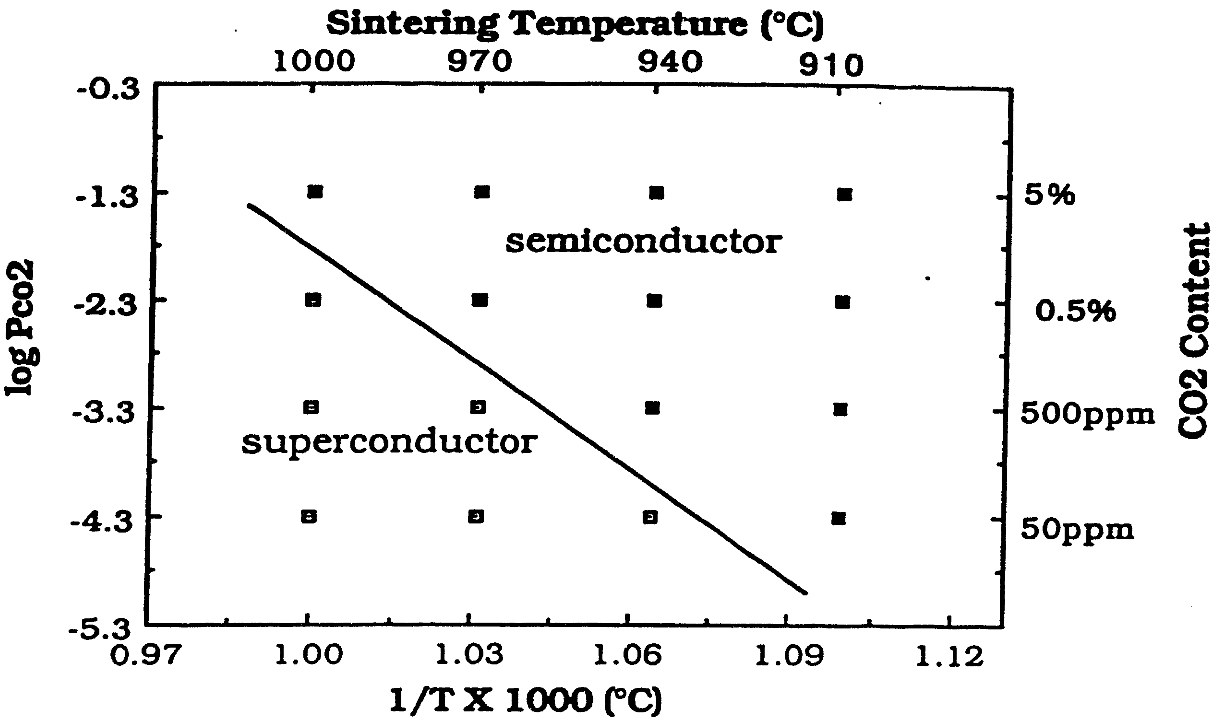
Sintering Temperature (°C)
1000
970
940
910
-0.3
-1.3
-2.3
-3.3
-4.3
-5.3
log Pco2
semiconductor
superconductor
5%
0.5%
500ppm
50ppm
CO2 Content
0.97
1.00
1.03
1.06
1.09
1.12
1/T X 1000 (°C)

Figure 1

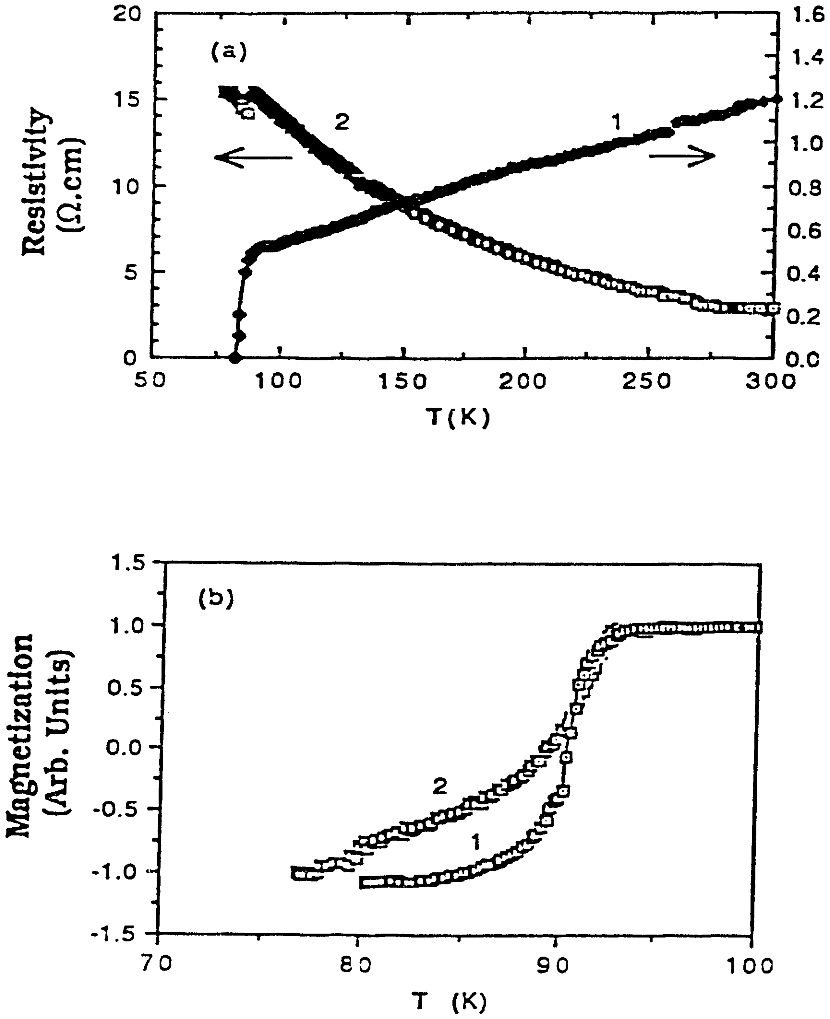
(a)
Resistivity (Ω.cm)
20
15
10
5
0
1.6
1.4
1.2
1.0
0.8
0.6
0.4
0.2
0.0
2
1
50
100
150
200
250
300
T(K)
(b)
Magnetization (Arb. Units)
1.5
1.0
0.5
0.0
-0.5
-1.0
-1.5
2
1
70
80
90
100
T (K)

(a)

(b)

Figure 2

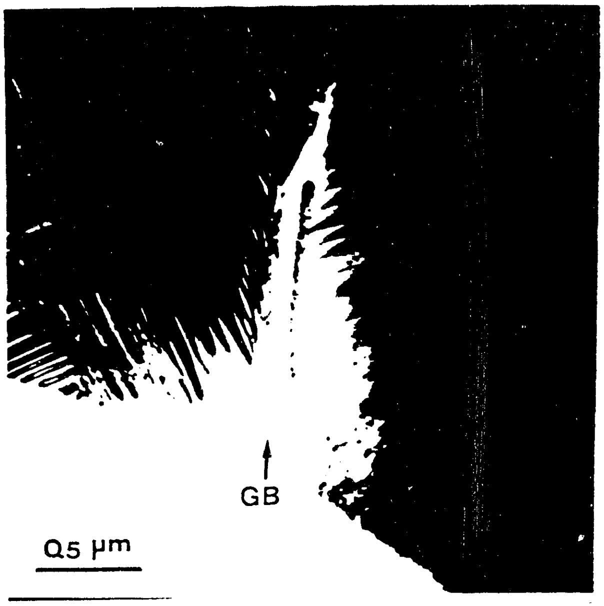

③

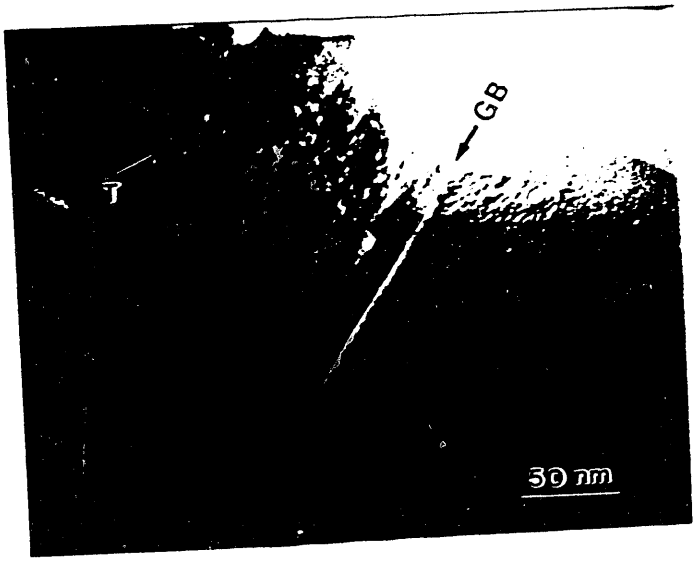

④

Figures 3 & 4

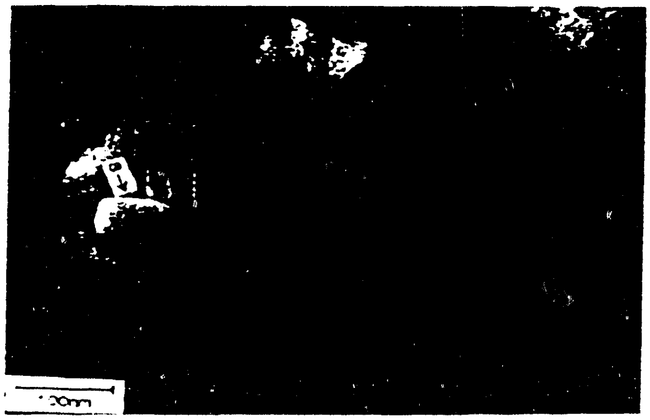

Figure 5

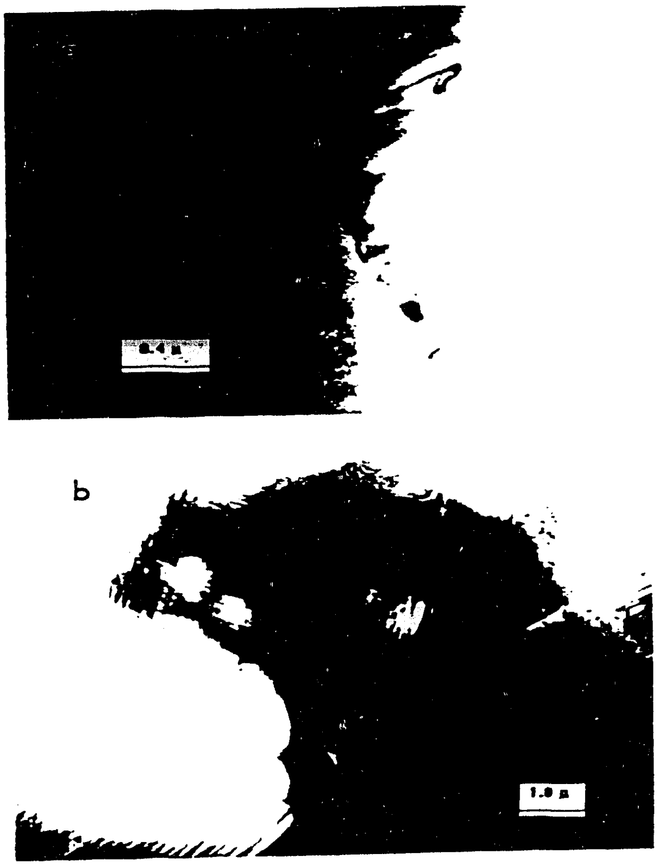

Figure 6

DATE
FILMED

1/12/94

END